HHS Public Access

Author manuscript

Colloids Surf B Biointerfaces. Author manuscript; available in PMC 2016 September 01.

Published in final edited form as:

Colloids Surf B Biointerfaces. 2016 September 1; 145: 122–129. doi:10.1016/j.colsurfb.2016.04.043.

Influence of chirality on catalytic generation of nitric oxide and platelet behavior on selenocystine immobilized TiO_2 films

Yonghong Fan[a,b], **Xiaxin Pan**[a,b], **Ke Wang**[a,b], **Sisi Wu**[a,b], **Honghong Han**[a,b], **Ping Yang**[a,b], **Rifang Luo**[a,b], **Hong Wang**[a,b], **Nan Huang**[a,b], **Wei Tan**[b], and **Yajun Weng**[a,b,*]

[a] Key Laboratory of Advanced Technologies of Materials, Ministry of Education, Southwest Jiaotong University, Chengdu 610031, China

[b] School of Materials Science and Engineering, Southwest Jiaotong University, Chengdu 610031, China

[c] Department of Mechanical Engineering, University of Colorado at Boulder, Boulder, CO 80309, USA

Abstract

As nitric oxide (NO) plays vital roles in the cardiovascular system, incorporating this molecule into cardiovascular stents is considered as an effective method. In the present study, selenocystine with different chirality (i.e., L- and D-selenocystine) was used as the catalytic molecule immobilized on TiO_2 films for decomposing endogenous NO donor. The influences of surface chirality on NO release and platelet behavior were evaluated. Results show that although the amount of immobilized L-selenocystine on the surface was nearly the same as that of immobilized D-selenocystine, in vitro catalytic NO release tests showed that L-selenocystine immobilized surfaces were more capable of catalyzing the decomposition of S-nitrosoglutathione and thus generating more NO. Accordingly, L-selenocystine immobilized surfaces demonstrated significantly increased inhibiting effects on the platelet adhesion and activation, when compared to D-selenocystine immobilized ones. Measurement of the cGMP concentration of platelets further confirmed that surface chirality played an important role in regulating NO generation and platelet behaviors. Additionally, using bovine serum albumin and fibrinogen as model proteins, the protein adsorption determined with quartz crystal microbalance showed that the L-selenocystine immobilized surface enhanced protein adsorption. In conclusion, surface chirality significantly influences protein adsorption and NO release, which may have significant implications in the design of NO-generating cardiovascular stents.

Keywords

Selenocystine; Chirality; Nitric oxide; Platelet activation

* Corresponding author at: Key Laboratory of Advanced Technologies of Materials, Ministry of Education, Southwest Jiaotong University, Chengdu 610031, China. wengyj7032@swjtu.edu.cn (Y. Weng).

Appendix A. Supplementary data

Supplementary data associated with this article can be found, in the online version, at http://dx.doi.org/10.1016/j.colsurfb.2016.04.043.

1. Introduction

It is widely accepted that the endothelial cell (EC), the cell that lines the inner wall of blood vessels, continuously produces and releases NO to sustain vascular patency [1]. The produced NO inhibits platelet adhesion, aggregation and activation, through the activation of soluble guanylate cyclase which catalyzes the conversion of guanosine 5′-triphosphate into cyclic guanylate monophosphate (cGMP) in platelet [2]. Also, NO plays a critical role in regulating blood pressure by limiting smooth muscle cells proliferation and leukocyte infiltration [3].

Numerous strategies have been explored to mimic EC functions and to improve hemocompatibility of cardiovascular implants. Among them, NO-releasing biomaterials show promising anti-coagulation property by dramatically reducing platelet adhesion and activation [4]. Incorporating NO donors into polymer coatings shows improved hemocompatibility [5]. However, the limitations of this approach include the early burst release of NO causing cytotoxicity [6] and the limited NO reserve for long-term release [7], which make it difficult to progress into clinical applications.

In the circulating blood in vivo, NO secreted by ECs rapidly converts into endogenous NO donors known as S-nitrosothiols (RSNOs), such as S-nitrosoglutathione (GSNO), S-nitrosocysteine (CysNO) and S-nitrosoalbumin (AlbNO), which are kept at a steady μM-level concentration in human plasma [1,3,8,9]. Glutathione peroxidase then catalyzes RSNO to generate NO in the presence of thiols [10,11]. Therefore, small molecules such as cystamine, cystine, selenocystamine and Cu^{2+}-cyclen have been immobilized on biomaterial surfaces to decompose RSNOs for NO production. Such biomaterials are called NO-generating materials [12,13]. Diselenide-immobilized surfaces are among those which display glutathione peroxidase-like catalytic activities [6,14]. We previously immobilized selenocystamine on the vascular stent, which successfully inhibited platelet adhesion and activation in vitro and reduced in-stent restenosis in vivo [15].

It was reported that chiral recognition and interaction regulated various biological processes at the interfaces of cells [16,17], tissues or organs [18]. Wang et al. [19] found that L-valine and D-valine grafted polymer showed different protein adsorption behaviors. Bandyopadhyay et al. [20] reported that the chiral monolayer of polyol-terminated alkanethiols exhibited a different resistance to protein adsorption and bacterial biofilm formation. Additionally, Nakano et al. [21] reported that chiral recognition at the heme active site of NO synthase was markedly enhanced by L-arginine and 5,6,7,8-tetrahydrobiopterin. These studies showed different biological performances of chiral biomaterials, which resulted from the interactions between chiral biointerface materials and biological systems. The surface chirality may also influence the catalytic activity of NO generating materials. In all these NO-generating studies, either achiral catalytic molecules or only one kind of chiral catalytic molecule was used. The influence of chirality on the catalytic activity or on the NO release remains elusive. In the present study, selenocystine with different chirality is used to build chiral surfaces for catalytic generation of NO. As TiO_2 film is a potential candidate for surface modification of cardiovascular implants [22], it was used as the substrate for the immobilization of L/D-selenocystine via a polydopamine

linker [23]. Because similar chiral carbon in L-selenocystine or D-selenocystine appears at two locations, the surface grafting of L-selenocystine or D-selenocystine with one of its amino group keeps the chirality of the outermost chiral carbon. Thus the chirality of the surface depends on the chiral selenocystine used. Scheme 1 illustrates L-selenocystine and D-selenocystine immobilized surfaces (L-Se and D-Se).

2. Materials and methods

2.1. Materials

UBMS450 high vacuum unbalanced magnetron sputtering system was used to deposit TiO_2 film onto the silicon (100) wafer. The deposited TiO_2 film was mainly anatase with a thickness of 300 nm. 3,4-Dihydroxyphenylalanine (dopamine), tris-base (Tris), S-nitrosoglutathione (GSNO), ethylenediamine-tetraacetic acid disodium salt (EDTA-2Na), L-glutathione (GSH), bovine serum albumin (BSA) and fibrinogen from human plasma were all purchased from Sigma-Aldrich Chemical Co. D-selenocystine and L-selenocystine were purchased from ChemPep Inc. and J&K Chemical Technology, respectively. Phosphate Buffered Saline (PBS, 0.01 M, pH = 7.4) was used in the NO release experiments.

2.2. Preparation of chiral surfaces by selenocystine immobilization

Silicon wafers with TiO_2 film coating were neatly cut into 8 mm × 8 mm squares as the substrates or 4 mm × 4 mm squares for NO release analysis. All samples were washed successively with acetone, ethanol and distilled water. Then the clean TiO_2 substrates were placed into a 24-well plate. The substrates with five layered polydopamine (PDM) was prepared as described in the literature [15]. Briefly, the first layer of polydopamine was grafted to the TiO_2 surface via immersion of the substrates in a 0.5 mL solution of 2 mg/mL dopamine (10 mM Tris buffer, pH = 8.5) at 37 °C with the lid open to allow water evaporation overnight. The substrates were sonicated for three times with 5 min in water each time to remove the weakly bonded dopamine. The five layers of polydopamine were thus built layer-by-layer on top of the substrate by repeating the process of incubation, evaporation and sonication.

The film of L-Se or D-Se was further immobilized on top of the polydopamine-grafted substrates. The L- or D-selenocystine solution was prepared by adding L- or D-selenocystine into 6 mM NaOH solution to reach a final selenocystine concentration of 3 mM. The polydopamine-grafted samples were then incubated in the L- or D-selenocystine solution at 37 °C for about 12 h. Finally, the samples were cleaned with distilled water three times to get rid of the unbounded selenocystine.

For in vitro stability analysis samples were incubated at 37 °C in PBS for 1 week, 3 weeks or 5 weeks by continuous shaking in an air bath oscillator incubator with 60 rpm.

2.3. Materials characterization

The chemical structures of the samples were characterized by an attenuated total reflectance Fourier transform infrared spectroscopy (ATR-FTIR, NICOLET 5700) with the diffuse reflectance mode in the range of 4000–400 cm^{-1}. X-ray photoelectron spectroscopy (XPS)

analysis was carried out by a PHI-5400 (PerkinElmer, USA) X-ray photoelectron spectrometer using a monochromatic AlKcx (hv = 1486.6 eV) at 10–20 kV working voltage and 45 mA emission current. The barometric pressure in the chamber was set below 2×10^{-9} Torr and the binding energy scale was standardized by setting the C1s peak at 284.6 eV. Static water contact angles of the samples were measured using the sessile drop method on a DSA100 contact angle instrument (KRÜSS, Germany).

2.4. NO release tests

A Sievers 280i chemiluminescence NO analyzer (NOA280i, GE, USA) was used to measure the catalytic generation of NO from GSNO [13] (Supporting information). Briefly, a 3 mL PBS solution containing 22 μM GSNO, 67 μM GSH, and 500 μM EDTA which chelates metal ion contaminants that might otherwise decompose RSNO, was added into the reaction vessel at 37 °C and protected from light. The sample was placed above the solution till the detecting baseline was steady. The sample was then pushed into the reaction vessel and the released NO was continuously purged from the test solution with nitrogen to the chemiluminescene analyzer. The resulting NO signal (gas phase in ppb) was recorded by a computer.

2.5. Protein adsorption on the surfaces

Quartz crystal microblance with dissipation (QCM-D) (Q-Sense AB, Sweden) was used to monitor the process of selenocystine immobilization and protein adsorption [24]. First, polydopamine was deposited onto the Au-coated single crystal sensor (10 mm diameter Au films). Subsequently, the polydopamine-deposited crystal sensors were inserted into the QCM-D instrument. PBS buffer was then pumped into the QCM-D's channels to run base lines. After the base lines were stable, the L- and D-selenocystine solutions were injected at a speed of 50 μL/min. When the QCM signals did not vary, PBS buffer was introduced into the channels again. Finally, when the signals were stable, BSA (0.1 mg/mL) was injected into the channels followed by washing with PBS buffer. Similarly, in another protein adsorption experiment, fibrinogen (0.1 mg/mL) was used to replace BSA.

2.6. In vitro platelet adhesion and cGMP analysis

Fresh whole blood was obtained legally from the Blood Center of Chengdu, China. The blood was centrifuged at 1500 rpm for 15 min to separate the blood corpuscle, from which the platelet rich plasma (PRP) was obtained [25]. Due to the instability of endogenous NO donors [1], almost no RSNO can be retained in the PRP. To study the NO effects on platelet adhesion, exogenous RSNO, GSNO and GSH, were added after the addition of 500 μL PRP to obtain a solution with 130 μM GSNO and 400 μM GSH. For the anti-collagen activation test, 10 μL collagen was also added to reach the final collagen concentration of 106 μg/mL. Another group in the platelet adhesion test has PRP as the only addition. The platelet adhesion study was performed by incubating the samples with or without GSNO or collagen in PRP at 37 °C for 30 min. After washed with PBS twice, they were fixed in 2.5% glutaraldehyde for 12 h and then rinsed with PBS for three times. The platelets adsorbed on the surfaces were dehydrated, stained with rhodamine, and then examined with a fluorescence microscope.

The cGMP of platelets was analyzed with human cGMP ELISA kit (Hufeng biotechnical Co., Shanghai, China) [26]. The process is similar to the GSNO-present platelet adhesion test in that PRP, GSNO and GSH were added onto the samples. After 30 min incubation, 100 μL of triton (10%) was added, which was followed by sonication for 10 min. The supernatant used for the analysis was obtained by precipitating the cell fragments with centrifugation at 2500 rpm for 10 min.

3. Results and discussion

3.1. Surface characterization

Fig. 1 shows the FTIR spectra of TiO_2, PDM and L-Se samples. Compared with TiO_2, the PDM sample shows two wide absorption peaks: one in the range of 3600 cm^{-1} and 2850 cm^{-1}, which is the overlap of O—H, N—H and C—H stretching absorption, and the other in the range of 1780 cm^{-1} and 1435 cm^{-1} which shows the overlap of benzene ring vibration, N H scissoring vibrations and C=O of quinone. In addition, a new peak is found at 1289 cm^{-1} when amplifying FTIR spectra at 400–1500 cm^{-1} the (Supporting information), which is the deformation vibration of O H and N H. Newly appearing on the L-Se sample are two peaks (1604 cm^{-1} and 1381 cm^{-1}) showing COO^- stretching vibration derived from the COO^- group of selenocystine.

As shown in Fig. 2a, the water contact angle of TiO_2 film is 77.6 ± 3.1°. After dopamine grafting, the water contact angle decreases to 60.7 ± 1.8°, because of the presence of hydrophilic functional groups including amines, quinone and phenol hydroxyl groups. After selenocystine immobilization, the water contact angle rises again because of the consumption of the hydrophilic functional groups such as quinone groups. There are no differences between L-Se (68.9 ± 1.4°) and D-Se (68.9 ± 1.1°), indicating that the surface chirality does not influence surface hydrophilicity [27]. However, differences in the water contact angle between the L-Se and D-Se samples are found after protein adsorption (Fig. 2b). Compared to D-Se, the L-Se sample is more hydrophilic after BSA adsorption, while it is slightly more hydrophobic after fibrinogen adsorption. The result suggest that the surface chirality may influence the protein adsorption which leads to the differences in surface hydrophilicity. BSA is known as a hydrophilic biomolecule and thus BSA adsorption enhances surface hydrophilicity [28]. Contrarily, it was reported that the water contact angle increased with fibrinogen adsorption [29]. Therefore, the fact that higher hydrophilicity of the L-Se sample after BSA adsorption and higher hydrophobicity after fibrinogen adsorption may both suggest its improved protein adsorption when compared to the D-Se sample.

The XPS was used to characterize the surface composition. Results show that the peak of nitrogen newly appears on the PDM sample (Fig. 3a), while peaks of selenium (Se 3d and Se LMM) are present on both Se samples. As full XPS spectrum of D-Se is just the same as that of L-Se, only L-Se is shown here.

No obvious differences exist in the high resolution XPS spectra of selenium between L-Se and D-Se, indicating that the two samples have similar amount of surface selenium content (Fig. 3b). After incubation in PBS for 1 week, 3 weeks or 5 weeks, the peak area of selenium for L-Se gradually decreases, suggesting gradual loss of selenium. Because the

peak position and shape do not change, the loss of surface selenium might be due to the removal of weakly bound selenocystine from the substrate.

3.2. Protein adsorption on L-Se and D-Se

QCM-D was used in our study to monitor molecule grafting or protein adsorption. The results are presented in Fig. 4 which shows selenocystine grafting onto polydopamine film with a density of 350 ng/cm^2. Although there is nearly no difference in the grafting amount between L-Se and D-Se according to the XPS analysis, BSA adsorption on L-Se (514 ng/cm^2) is much higher than that on D-Se (403 ng/cm^2) (Fig. 4a). The same absorption phenomenon was also observed when fibrinogen was used as the model protein (Fig. 4b).

QCM-D analysis also shows that the L-Se surface promotes more protein adsorption, which is consistent with the literature [19]. The adsorption of proteins on biomaterial surfaces is generally considered as an 'inevitable' process. The process is driven by various interdependent interactions such as hydrogen bonding, steric, electrostatic and hydrophobic interactions [30,31]. In the present study, the L-Se and D-Se surfaces are both negatively charged due to the addition of NaOH to dissolve selenocystine. As BSA and fibrinogen are both negatively charged, electrostatic repulsion prevents the two proteins from attaching to the L-Se or D-Se surfaces. The main driving forces for the adsorption of both proteins may be attributed to hydrogen bonding and hydrophobic interaction [19]. The difference of steric structure of L-Se and D-Se may lead to different steric interactions, which in turn influence hydrogen bonding and hydrophobic interaction. Endogenous NO donor GSNO was not used in the QCM adsorption detection, because the GSNO adsorption on these surfaces can lead to NO release which interferes the QCM detection.

3.3. Catalytic generation of NO in vitro

Chemiluminescence analysis provides an accurate means of NO detection. A Sievers 280i chemiluminescence NO analyzer was used here to evaluate NO release, as done in previous studies [6,32,33]. The NO production catalyzed by L-Se or D-Se exhibited a steady release speed as a zero-order reaction (Fig. 5). A high noise peak can be seen when the GSNO solution was injected or when the sample was pushed into the reaction solution which caused flow disturbance. Although there is nearly no difference in terms of the amount of immobilized selenocystine between L-Se and D-Se, a significant difference of NO flux between the two samples was found: NO generation catalyzed by L-Se (11.25 ± 1.22 ppb) was much faster than that catalyzed by D-Se (7.83 ± 1.59 ppb) (Fig. 5a). After 1 week, 3 weeks or 5 weeks of incubation in PBS, the difference still existed while the NO release from each sample decreased slightly with the prolonged incubation (Fig. 5b). Results from the present study are in good agreement with previous studies which showed that the surfaces immobilized with L-amino acid improved protein adsorption regardless of the protein type [19,34]. Compared to D-Se, the L-Se sample also likely promotes the adsorption of GSNO, a nitro derivative of GSH which is a protein fragment [35]. Upon adsorption on the surface, GSNO is immediately consumed to produce NO, and thus the process of GSNO adsorption converts into the mass transfer. Different from the protein adsorption in equilibrium with desorption from a surface, GSNO is continuously transferred to a surface due to the constant consumption, which is driven by the intermolecular force similar to

protein adsorption. Even though there is no difference in the surface selenium content or the amount of catalytic active sites between L-Se and D-Se samples, the GSNO decomposition or the NO release is enhanced on the L-Se, due to faster transfer of GSNO.

3.4. In vitro platelet adhesion and cGMP analysis

The effect of immobilized chiral molecules on the platelet adhesion was also investigated. As the injury of vascular endothelium due to stent implantation always leads to collagen exposure, collagen was used as an activator in the study [36–38]. Two groups, one with PRP and collagen and the other with PRP only, were included in the study. It is known that platelets adsorbed on biomaterial surfaces can exhibit five different morphologies, i.e., round, dendritic, spread dendritic, spreading and fully spreading shapes [39]. As shown in Fig. 6, when PRP and collagen were both added onto the samples, the morphology of platelets adhered on the PDM sample was more spreading with more aggregates compared with those on TiO_2. Results also showed that the platelet adhesion, aggregation and activation on D-Se was lower than those on L-Se. When the GSNO solution was also added, the number of adhered and activated platelets decreased dramatically on L-Se and D-Se, which can be attributed to the NO release through the GSNO self-decomposition which has a half time of about 8 min in the physiological condition [1]. Quantitative analysis showed that the number and the spreading area of adhered platelets on L-Se were the lowest among all samples (Fig. 7). Platelets on L-Se were mostly round while some platelets on D-Se showed spreading morphology. Because the NO release on L-Se was higher than that on D-Se, results here suggest that continuous NO release helped to inhibit collagen-induced platelet activation. Furthermore, in the presence of GSNO, compared with TiO_2, the platelet adhesion significantly decreased on PDM whose quinone residues might speed up GSNO decomposition [40].

Blood platelet activation is critical to homeostasis, since inappropriate platelet activation leads to thrombosis. It is known that NO can act as the platelet activation inhibitor through activating soluble guanylate cyclase, an enzyme that synthesizes cGMP [41]. Therefore, as a secondary messenger of NO release, the levels of cGMP in platelet should be associated with the NO release. Fig. 8 shows the concentration of cGMP synthesized by platelets attached to different samples. The result reveals that cGMP in plasma increased after incubation with both L-Se and D-Se, while the cGMP concentration with L-Se were significantly higher when compared with that with D-Se.

The highly diffusible nature of NO allows it to enter the platelet, where it activates guanylate cyclase, leading to a rapid increase in the cGMP concentration [42]. As NO releasing speed catalyzed by L-Se was enhanced, the cGMP concentration of platelet incubated with L-Se was found to be the highest while the activated degree of the adhered platelets was the least when endogenous NO donor was added. Although it was reported that NO inhibited platelet adhesion or activation to collagen through cGMP-independent mechanisms [43,44], the present study shows that the inhibition of platelet activation through NO release is positively correlated with the cGMP concentration. Thus, surface chirality influences platelet behavior by varying NO releasing speed. Overall, this study suggests that L-Se may have better hemocompatibility than D-Se.

4. Conclusion

In the present study, small chiral molecules of selenocystine were immobilized on TiO_2 via a polydopamine linker. Both XPS and QCM analyses show L-Se or D-Se surfaces have similar surface composition and the same amount of immobilized selenocystine. Water contact angle analysis also shows both surfaces have similar hydrophilicity. Despite these similarities, the two surfaces are quite different in their biological performances. After protein adsorption, an obvious difference in surface hydrophilicity between the two surfaces was found. QCM detection confirms L-Se promotes more protein adsorption. NO release analysis shows that NO generation is enhanced by L-Se. Therefore, L-Se is also found to be more capable of inhibiting platelet adhesion and activation.

Supplementary Material

Refer to Web version on PubMed Central for supplementary material.

Acknowledgments

The financial support for this work by National Natural Science Foundation of China (No. 31270020), Key Basic Research Project (No. 2011CB606204), Sichuan Province Science Foundation for Youths (No. 2013JQ0043), Fundamental Research Funds for the Central Universities (2682014CX006) and NIH (NHLBI 119371 to W. Tan) are greatly acknowledged.

References

[1]. Kelm M. Nitric oxide metabolism and breakdown. Biochim. Biophys. Acta. 1411(1999):273–289. [PubMed: 10320663]

[2]. Moncada S, Palmer RM, Higgs EA. Nitric oxide: physiology, pathophysiology, and pharmacology. Pharmacol. Rev. 43(1991):109–142. [PubMed: 1852778]

[3]. Yang Y, Qi P, Wen F, Li X, Xia Q, Maitz MF, Yang Z, Shen R, Tu Q, Huang N. Mussel-inspired one-step adherent coating rich in amine groups for covalent immobilization of heparin: hemocompatibility, growth behaviors of vascular cells, and tissue response. ACS Appl. Mater. Inter. 6(2014):14608–14620.

[4]. de Mel A, Murad F, Seifalian AM. Nitric oxide: a guardian for vascular grafts? Chem. Rev. 111(2011):5742–5767. [PubMed: 21663322]

[5]. Bohl KS, West JL. Nitric oxide-generating polymers reduce platelet adhesion and smooth muscle cell proliferation. Biomaterials. 21(2000):2273–2278. [PubMed: 11026633]

[6]. Cha W, Meyerhoff ME. Catalytic generation of nitric oxide from S-nitrosothiols using immobilized organoselenium species. Biomaterials. 28(2007):19–27. [PubMed: 16959311]

[7]. Naghavi N, de Mel A, Alavijeh OS, Cousins BG, Seifalian AM. Nitric oxide donors for cardiovascular implant applications. Small. 9(2013):22–35. [PubMed: 23136136]

[8]. Goldman RK, Vlessis AA, Trunkey DD. Nitrosothiol quantification in human plasma. Anal. Biochem. 259(1998):98–103. [PubMed: 9606149]

[9]. Ng ES, Kubes P. The physiology of S-nitrosothiols: carrier molecules for nitric oxide. Can. J. Physiol. Pharmacol. 81(2003):759–764. [PubMed: 12897804]

[10]. Freedman JE, Frei B, Welch GN, Loscalzo J. Glutathione peroxidase potentiates the inhibition of platelet function by S-nitrosothiols. J. Clin. Invest. 96(1995):394–400. [PubMed: 7615810]

[11]. Hou YC, Li J, Wang PG. Seleno compounds and glutathione peroxidase catalyzed decomposition of S-nitrosothiols. Biochem Biophys. Res. Commun. 228(1996):88–96. [PubMed: 8912640]

[12]. Duan X, Lewis RS. Improved haemocompatibility of cysteine-modified polymers via endogenous nitric oxide. Biomaterials. 23(2002):1197–1203. [PubMed: 11791923]

[13]. Yang J, Welby JL, Meyerhoff ME. Generic nitric oxide (NO) generating surface by immobilizing organoselenium species via layer-by-layer assembly. Langmuir. 24(2008):10265–10272. [PubMed: 18710268]

[14]. Chaudiere J, Courtin O, Leclaire J. Glutathione oxidase activity of selenocystamine: a mechanistic study. Arch. Biochem. Biophys. 296(1992):328–336. [PubMed: 1605642]

[15]. Weng Y, Song Q, Zhou Y, Zhang L, Wang J, Chen J, Leng Y, Li S, Huang N. Immobilization of selenocystamine on TiO_2 surfaces for in situ catalytic generation of nitric oxide and potential application in intravascular stents. Biomaterials. 32(2011):1253–1263. [PubMed: 21093045]

[16]. Sun T, Han D, Riehemann K, Chi L, Fuchs H. Stereospecific interaction between immune cells and chiral surfaces. J. Am. Chem. Soc. 129(2007):1496–1497. [PubMed: 17283984]

[17]. Li M, Qing G, Zhang M, Sun T. Chiral polymer-based biointerface materials. Sci. Chin. Chem. 57(2014):540–551.

[18]. Zhang M, Qing G, Sun T. Chiral biointerface materials. Chem. Soc. Rev. 41(2012):1972–1984. [PubMed: 22138816]

[19]. Wang X, Gan H, Sun T. Chiral design for polymeric biointerface: the influence of surface chirality on protein adsorption. Adv. Funct. Mater. 21(2011):3276–3281.

[20]. Bandyopadhyay D, Prashar D, Luk YY. Anti-fouling chemistry of chiral monolayers: enhancing biofilm resistance on racemic surface. Langmuir. 27(2011):6124–6131. [PubMed: 21486002]

[21]. Nakano K, Sagami I, Daff S, Shimizu T. Chiral recognition at the heme active site of nitric oxide synthase is markedly enhanced by l-arginine and 5,6,7,8-tetrahydrobiopterin. Biochem. Biophys. Res. Commun. 248(1998):767–772. [PubMed: 9704002]

[22]. Huang N, Yang P, Leng YX, Chen JY, Sun H, Wang J, Wang GJ, Ding PD, Xi TF, Leng Y. Hemocompatibility of titanium oxide films. Biomaterials. 24(2003):2177–2187. [PubMed: 12699653]

[23]. Lee BP, Messersmith PB, Israelachvili JN, Waite JH. Mussel-inspired adhesives and coatings. Annu. Rev. Mater. Res. 41(2011):99–132. [PubMed: 22058660]

[24]. Lin Q, Ding X, Qiu F, Song X, Fu G, Ji J. In situ endothelialization of intravascular stents coated with an anti-CD34 antibody functionalized heparin-collagen multilayer. Biomaterials. 31(2010): 4017–4025. [PubMed: 20149438]

[25]. Liu Y, Luo R, Shen F, Tang L, Wang J, Huang N. Construction of mussel-inspired coating via the direct reaction of catechol and polyethyleneimine for efficient heparin immobilization. Appl. Surf. Sci. 328(2015):163–169.

[26]. Yang Z, Yang Y, Xiong K, Li X, Qi P, Tu Q, Jing F, Weng Y, Wang J, Huang N. Nitric oxide producing coating mimicking endothelium function for multifunctional vascular stents. Biomaterials. 63(2015):80–92. [PubMed: 26093790]

[27]. Wang X, Gan H, Zhang M, Sun T. Modulating cell behaviors on chiral polymer brush films with different hydrophobic side groups. Langmuir. 28(2012):2791–2798. [PubMed: 22216960]

[28]. Wei Q, Li B, Yi N, Su B, Yin Z, Zhang F, Li J, Zhao C. Improving the blood compatibility of material surfaces via biomolecule-immobilized mussel-inspired coatings. J. Biomed. Mater. Res. A. 96(2011):38–45. [PubMed: 20949483]

[29]. Weber N, Pesnell A, Bolikal D, Zeltinger J, Kohn J. Viscoelastic properties of fibrinogen adsorbed to the surface of biomaterials used in blood-contacting medical devices. Langmuir. 23(2007):3298–3304. [PubMed: 17291015]

[30]. Salloum DS, Schlenoff JB. Protein adsorption modalities on polyelectrolyte multilayers. Biomacromolecules. 5(2004):1089–1096. [PubMed: 15132703]

[31]. Qing G, Sun T. Chirality-triggered wettability switching on a smart polymer surface. Adv. Mater. 23(2011):1615–1620. [PubMed: 21472788]

[32]. Hwang S, Meyerhoff ME. Polyurethane with tethered copper(II)-cyclen complex: preparation, characterization and catalytic generation of nitric oxide from S-nitrosothiols. Biomaterials. 29(2008):2443–2452. [PubMed: 18314189]

[33]. Oh BK, Meyerhoff ME. Catalytic generation of nitric oxide from nitrite at the interface of polymeric films doped with lipophilic Cu(II)-complex: a potential route to the preparation of thromboresistant coatings. Biomaterials. 25(2004):283–293. [PubMed: 14585716]

[34]. Zhou F, Yuan L, Li D, Huang H, Sun T, Chen H. Cell adhesion on chiral surface: the role of protein adsorption. Colloids Surf. B. 90(2012):97–101.

[35]. Broniowska KA, Diers AR, Hogg N. S-nitrosoglutathione. Biochim. Biophys. Acta. 1830(2013): 3173–3181. [PubMed: 23416062]

[36]. Nuyttens BP, Thijs T, Deckmyn H, Broos K. Platelet adhesion to collagen. Thromb. Res. 2011; 127:S26–S29.

[37]. Vanhoorelbeke K, Ulrichts H, Schoolmeester A, Deckmyn H. Inhibition of platelet adhesion to collagen as a new target for antithrombotic drugs. Curr. Drug Target Cardiovasc. Hematol. Disord. 3(2003):125–140.

[38]. Farndale RW. Collagen-induced platelet activation. Blood Cells Mol. Dis. 36(2006):162–165. [PubMed: 16464621]

[39]. Goodman SL, Grasel TG, Cooper SL, Albrecht RM. Platelet shape change and cytoskeletal reorganization on polyurethaneureas. J. Biomed. Mater. Res. 23(1989):105–123. [PubMed: 2708401]

[40]. Alegria AE, Dejesus-Andino FJ, Sanchez-Cruz P. Quinone-enhanced sonochemical production of nitric oxide from s-nitrosoglutathione. Ultrason. Sonochem. 16(2009):190–196. [PubMed: 18595761]

[41]. Thatcher GR, Nicolescu AC, Bennett BM, Toader V. Nitrates and NO release: contemporary aspects in biological and medicinal chemistry. Free Radical Biol. Med. 37(2004):1122–1143. [PubMed: 15451053]

[42]. Schmidt HH, Lohmann SM, Walter U. The nitric oxide and cGMP signal transduction system: regulation and mechanism of action. Biochim. Biophys. Acta. 1178(1993):153–175. (BBA). [PubMed: 7688574]

[43]. Hirst, DG.; Robson, T. Nitric oxide physiology and pathology. In: McCarthy, OH.; Coulter, AJ., editors. Nitric Oxide: Methods and Protocols. Humana Press; Totowa, NJ: 2011. p. 1-13.

[44]. Rukoyatkina N, Walter U, Friebe A, Gambaryan S. Differentiation of cGMP-dependent and -independent nitric oxide effects on platelet apoptosis and reactive oxygen species production using platelets lacking soluble guanylyl cyclase. Thromb. Haemost. 106(2011):922–933. [PubMed: 21800013]

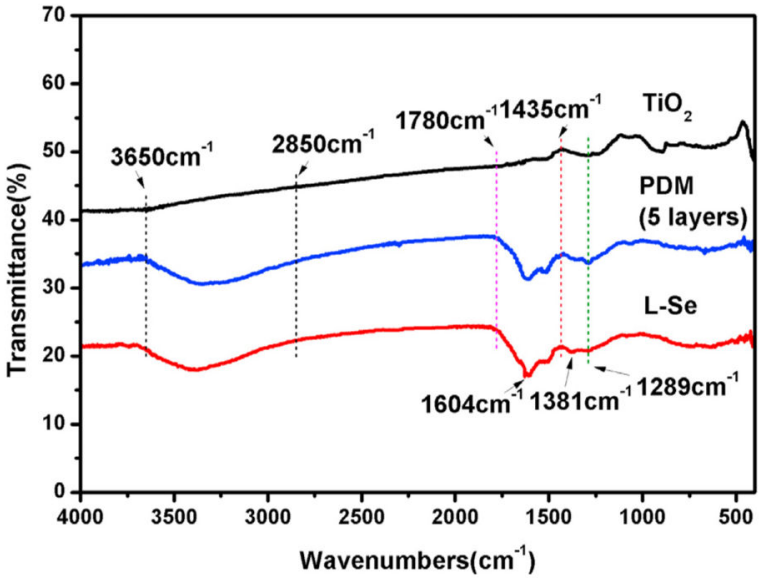

Fig. 1.
FTIR spectra of TiO_2 film, PDM film and L-Se sample.

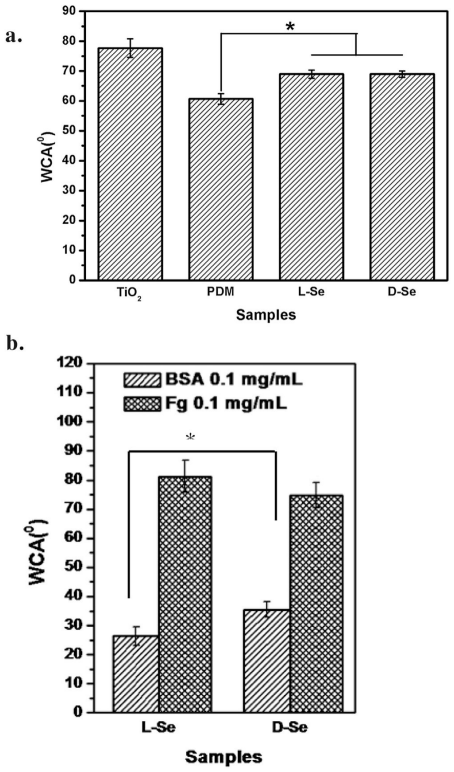

Fig. 2.

The water contact angle (WCA) of freshly prepared samples (a) and L-Se and D-Se samples after protein adsorption of fibrinogen (Fg) or BSA (b). Data are presented as mean ± SD ($n \geq 6$). "*" shows $p < 0.05$.

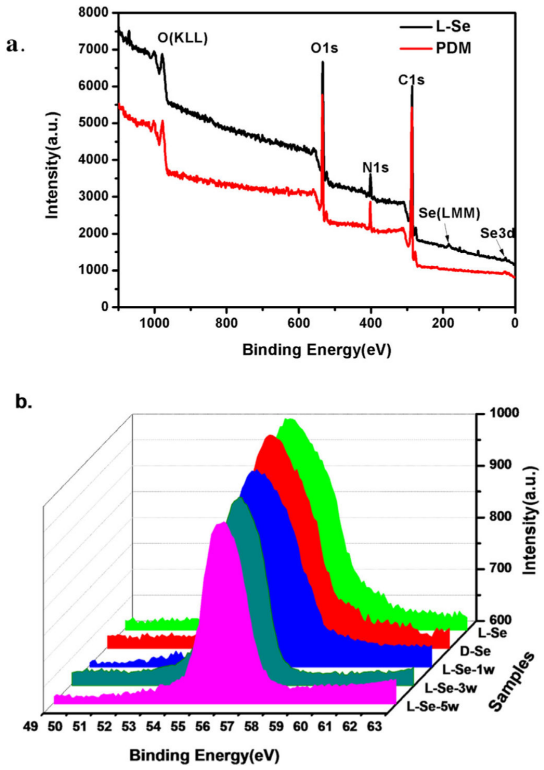

Fig. 3.

XPS spectra. (a) Spectra of the L-Se sample and PDM film. (b) The Se high resolution XPS spectra of L-Se, D-Se and samples incubated in PBS for 1 week, 3 weeks or 5 weeks.

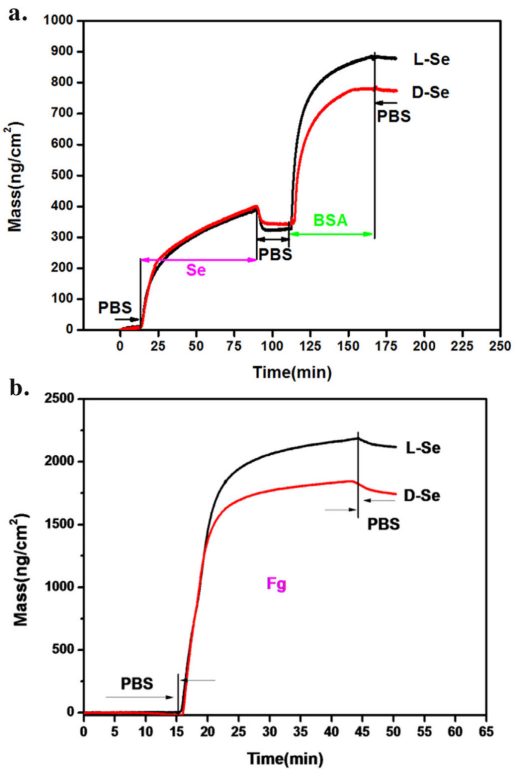

Fig. 4.

QCM-D detection of the mass dynamics, showing (a) selenocystine (3 mM) grafting on the polydopamine linker, followed by BSA (0.1 mg/mL) adsorption, and (b) fibrinogen (0.1 mg/mL) adsorption on L-Se or D-Se surfaces.

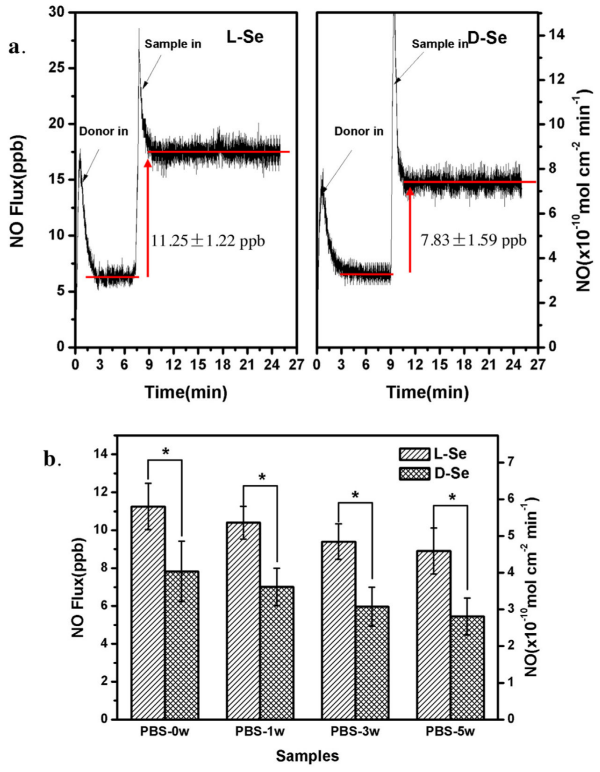

Fig. 5.

Release rates of NO catalytically generated by L-Se and D-Se samples in fresh PBS (3 mL, pH = 7.4) containing NO donor of 22 mM GSNO, 67 mM GSH and 500 mM EDTA. (a) NO flux curves of L-Se and D-Se; (b) NO release rates of the samples incubated in PBS for 0, 1, 3 or 5 weeks. Data are presented as mean ± SD ($n \geq 4$). "*" shows $p < 0.05$.

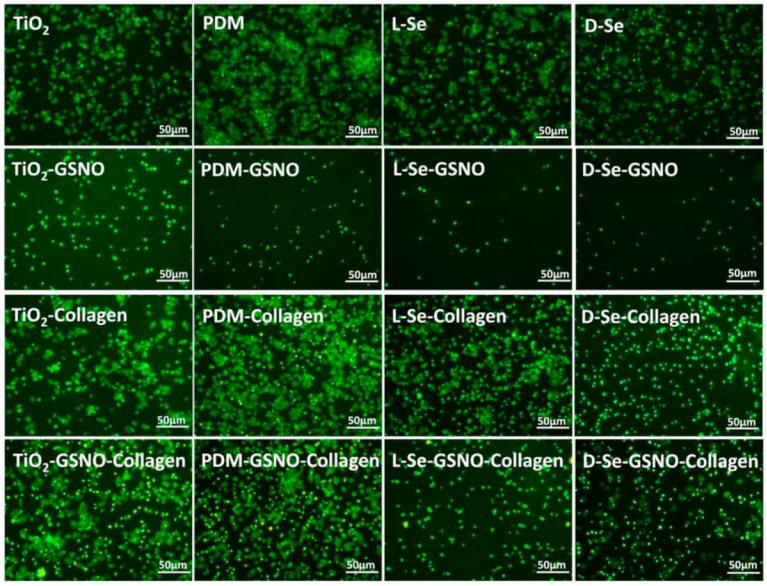

Fig. 6.

Immunofluoresent images showing the platelet adhesion on TiO_2, PDM, L-Se or D-Se with or without GSNO or collagen after incubation with PRP at 37 ° C for 30 min.

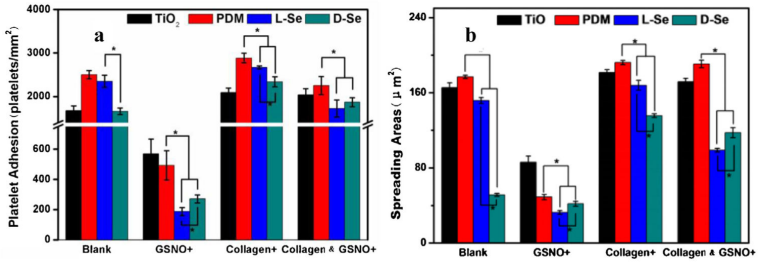

Fig. 7.

Quantitative measures of platelet adhesion: (a) the number of adhered platelets, and (b) the spreading area of adhered platelets on TiO_2, PDM, L-Se and D-Se. Data are presented as mean ± SD ($n \geq 4$). "*" shows $p < 0.05$.

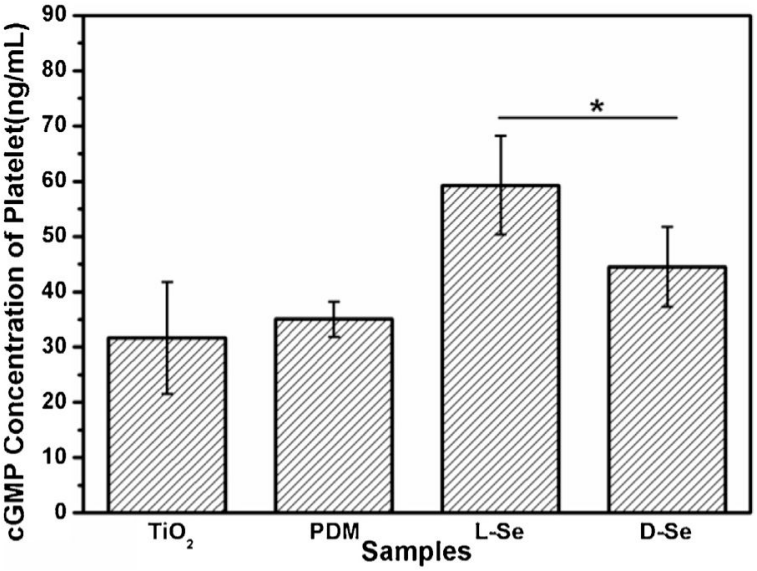

Fig. 8.

The concentration of cGMP synthesized by platelets incubated with TiO_2, PDM, L-Se and D-Se in the presence of GSNO and GSH for 30 min at 37 ° C. Data are presented as mean ± SD ($n \geq 4$). "*" shows $p < 0.05$.

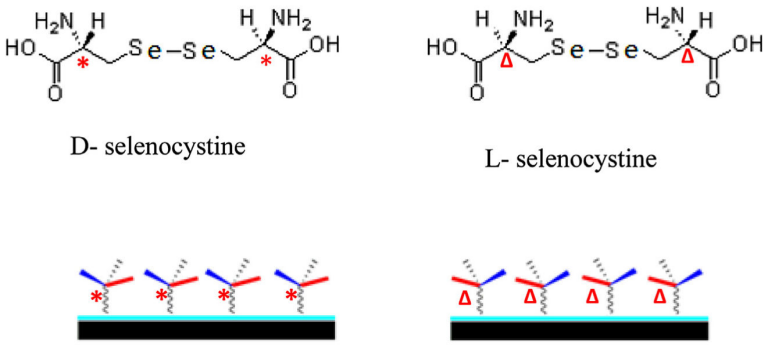

Scheme 1.

Schematic figure of L-and D-selenocystine immobilization on TiO_2 films via a polydopamine linker to form chiral surfaces (*: chiral center of D-selenocystine; Δ:chiral center of L-selenocystine).